JOC The Journal of Organic Chemistry
Cite This: J. Org. Chem. 2019, 84, 2808−2816
Article
pubs.acs.org/joc

# Shape-Selective Recognition of Quaternary Ammonium Chloride Ion Pairs

Dong-Hao Li and Bradley D. Smith*

Department of Chemistry and Biochemistry, University of Notre Dame, 236 Nieuwland Science Hall, Notre Dame, Indiana 46556, United States

Supporting Information

**ABSTRACT:** Synthetic receptors that recognize ion pairs are potentially useful for many technical applications, but to date there has been little work on selective recognition of quaternary ammonium ($Q^+$) ion pairs. This study measured the affinity of a tetralactam macrocycle for 11 different $Q^+ \cdot Cl^-$ salts in chloroform solution. In each case, NMR spectroscopy was used to determine the association constant ($K_a$) and the structure of the associated complex. $K_a$ was found to depend strongly on the molecular shape of $Q^+$ and was enhanced when $Q^+$ could penetrate the macrocycle cavity and engage in attractive noncovalent interactions with the macrocycle's NH residues and aromatic sidewalls. The highest measured $K_a$ of 7.9 × $10^3$ $M^{-1}$ was obtained when $Q^+$ was a *p*-CN-substituted benzylic trimethylammonium. This high-affinity $Q^+ \cdot Cl^-$ ion pair was used as a template to enhance the synthetic yield of macrocyclization reactions that produce the tetralactam receptor or structurally related derivatives. In addition, a permanently interlocked rotaxane was prepared by capping the end of a noncovalent complex composed of the tetralactam macrocycle threaded by a reactive benzylic cation. The synthetic method provides access to a new family of rotaxanated ion pairs that can likely act as anion sensors, molecular shuttles, or transport molecules.

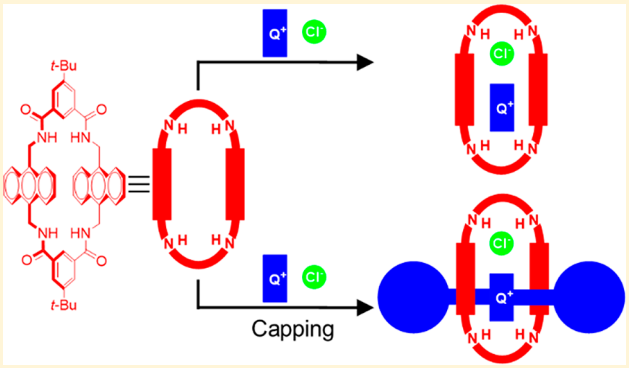


## INTRODUCTION

Synthetic receptors that recognize ion pairs are potentially useful for many technical applications including purification, templated synthetic chemistry, catalysis, membrane transport, and drug delivery.[1−7] To date, most of the effort has focused on receptors that recognize alkali or alkaline metal salts as either contact or separated ion pairs. The goal of many published studies has been to develop heteroditopic receptors with distinct anion and cation sites and to show that they exhibit positive binding cooperativity.[8] One example of positive cooperativity, that is relevant to this report, is when the association constant, $K_a$, for anion binding to a heteroditopic receptor is increased by simultaneous binding of a proximal cation.[9] This type of positive binding cooperativity seems intuitive since the cation and anion guests are attracted electrostatically. But as discussed by others, ion-pair recognition in weakly polar solvents can be quite a complicated phenomenon involving several competing equilibria.[10,11]

The community focus on alkali or alkaline metal salts is understandable since they have a high charge-to-surface ratio and a strong propensity to form ion pairs in weakly polar solvents. In contrast, quaternary ammonium cations have a much lower charge-to-surface ratio and are often treated as diffuse cations that do not favor ion pairs.[12] Indeed, most studies of anion binding in organic solvents use tetrabutylammonium ($TBA^+$) salts with the assumption that there is negligible interaction between the anion and the $TBA^+$ countercation.[13] However, quaternary ammonium salts are known to form weak ion pairs in nonpolar solvents, and there are a few published reports of receptor systems that bind quaternary ammonium or alkylpyridinium salts as ion pairs.[14−19] A common structural feature of these literature heteroditopic receptor molecules is an aromatic surface to interact with the organic cation and a separate set of hydrogen donors for anion binding,[20−25] but to the best of our knowledge, there has been no systematic study showing how anion affinity can enhanced by changing the identity of a quaternary ammonium cation.

Here, we report that the $Cl^-$ binding ability of macrocyclic receptor **M** (Scheme 1a) in chloroform solution depends strongly on the structural shape of the counter quaternary ammonium cation, $Q^+$. We first disclosed **M** in 2007 and showed that its macrocyclic structure is highly preorganized with the four NH residues directed inward toward the macrocyclic cavity (Scheme 1b).[26,27] We have previously demonstrated that **M** has high binding affinities for various

Received: December 17, 2018
Published: February 7, 2019






DOI: 10.1021/acs.joc.8b03197
J. Org. Chem. 2019, 84, 2808−2816

**Scheme 1. (a) Chemical Structures of Receptor M and the Quaternary Ammonium Chloride That Salts Were Studied as Guests; Cartoon Representations of (b) Empty M, (c) $Cl^-$@M, and (d) $Q^+$·$Cl^-$@M; (e) Energy-Minimized Structure (Semiempirical, PM7) of $TBA^+$·$Cl^-$@M with $TBA^+$ Deleted for Clarity**

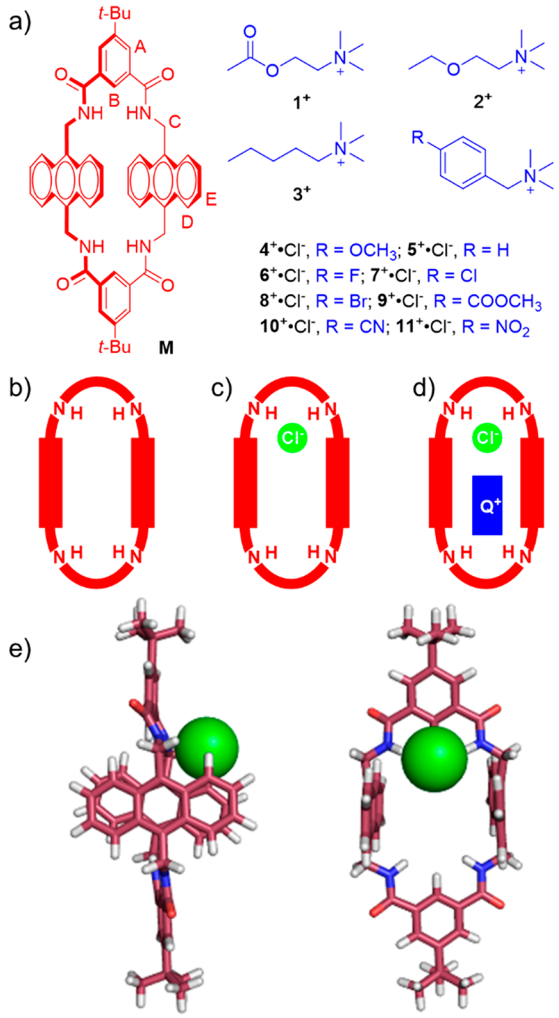


squaraine dyes, and more recently, we discovered that **M** also has high affinities for several anionic square planar coordination complexes of precious metals.[28] During these projects, we noted that **M** binds $Cl^-$ with unusually weak affinity. Molecular modeling suggests that the bound $Cl^-$ is perched outside the cavity of **M** to avoid repulsive interactions with the electron-rich cavity (which is lined with anthracene sidewalls) and that there is essentially no interaction of **M** or $Cl^-$ with the diffuse $TBA^+$ (Scheme 1c,e).

We wondered if the $Cl^-$ binding ability of **M** could be enhanced if the $TBA^+$ was replaced with a quaternary ammonium cation, $Q^+$, that had the structural shape and functionality to interact with the internal cavity of **M**.[29] As a starting hypothesis, we assumed that the $Cl^-$ would occupy two of the NH residues in **M**, and thus, the remaining two NH residues and the aromatic sidewalls of the macrocycle's cavity would be available for noncovalent interactions with $Q^+$ (see Scheme 1d). The hypothesis was tested by conducting a series of NMR titration experiments that added the 11 different $Q^+$·$Cl^-$ salts shown in Scheme 1a. The structures of the $Q^+$ component contained different functional groups, such as hydrogen-bond acceptors and aromatic surfaces, that could potentially interact with the functionality within the cavity of **M**. In some cases, there is clear evidence that $Q^+$ penetrates the cavity of **M** and induces a large increase in $Cl^-$ affinity (i.e., positive binding cooperativity). The practical value of this finding is demonstrated by (a) employing a high affinity $Q^+$·$Cl^-$ guest as an ion-pair template to greatly enhance the yields of macrocyclization reactions that make **M** or structurally related derivatives and (b) conducting a capping reaction that creates a new type of rotaxanated ion pair.

## RESULTS AND DISCUSSION

**NMR Studies of Association.** All of the following NMR studies were conducted in $CDCl_3$, and thus, an additional criterion for choice of $Q^+$·$Cl^-$ beyond its molecular structure was good solubility at millimolar concentration. The first set of $^1H$ NMR studies simply acquired spectra of **M** in the presence of 1 molar equiv of $Q^+$ salts. In all cases, the spectral patterns were consistent with either no interaction or an association process that was rapid on the NMR time scale.

Figures 1 and 2 show spectra for different samples containing acetylcholine salts where $Q^+$ = $\mathbf{1}^+$ and the

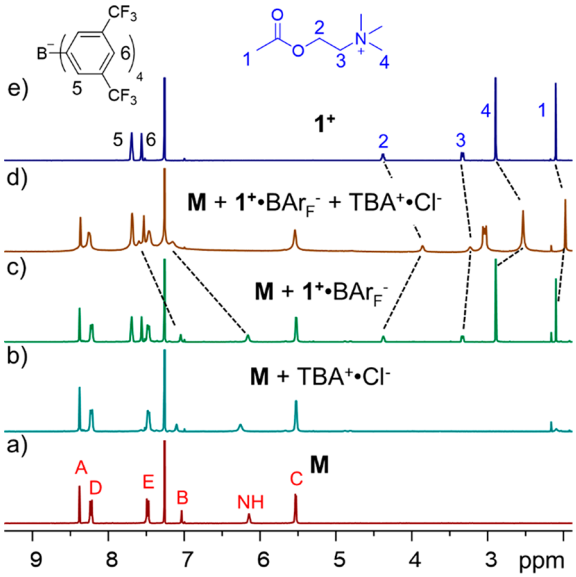


**Figure 1.** Partial $^1H$ NMR spectra (400 MHz, $CDCl_3$, 1 mM, 25 °C) of (a) **M**, (b) equimolar mixture of **M** and $TBA^+$·$Cl^-$, (c) equimolar mixture of **M** and $\mathbf{1}^+$·$BAr_F^-$, (d) equimolar mixture of **M**, $\mathbf{1}^+$·$BAr_F^-$, and $TBA^+$·$Cl^-$, and (e) $\mathbf{1}^+$·$BAr_F^-$. Atom labels for **M** are provided in Scheme 1.

counteranion is $Cl^-$ or $BAr_F^-$ ($BAr_F^-$ = tetrakis[3,5-bis-(trifluoromethyl)phenyl]borate). A comparison of the spectra for free **M** (Figure 1a), $\mathbf{1}^+$·$BAr_F^-$ (Figure 1e) and a 1:1 mixture of **M** + $\mathbf{1}^+$·$BAr_F^-$ (Figure 1c) shows no change in chemical shifts indicating no interaction of **M** with $\mathbf{1}^+$ or $BAr_F^-$. In contrast, a comparison of the spectra for free **M**, $\mathbf{1}^+$·$Cl^-$ and a 1:1 mixture of **M** + $\mathbf{1}^+$·$Cl^-$ (Figure 2) shows complexation-induced changes in chemical shifts. Specifically, there are upfield changes in chemical shifts for all protons in $\mathbf{1}^+$ and downfield changes in chemical shift for the NH residues and protons B of **M**. These changes indicate hydrogen bonding between **M** and $Cl^-$ and inclusion of $\mathbf{1}^+$ inside the cavity of **M**. Independent confirmation that $\mathbf{1}^+$ was inside the cavity of **M** was gained by observing cross-relaxation peaks in the ROESY


DOI: 10.1021/acs.joc.8b03197
J. Org. Chem. 2019, 84, 2808−2816

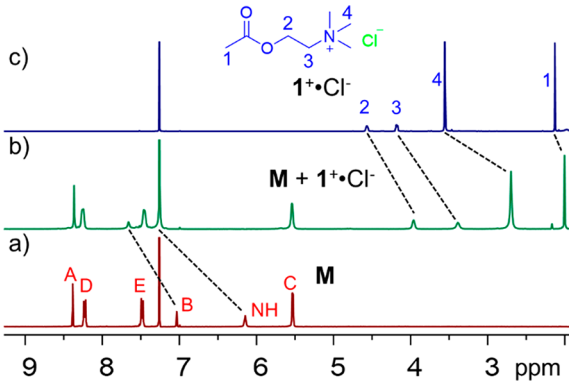


**Figure 2.** Partial $^1$H NMR spectra (400 MHz, $CDCl_3$, 1 mM, 25 °C) of (a) **M**, (b) equimolar mixture of **M** and $\mathbf{1}^+\cdot Cl^-$, and (c) $\mathbf{1}^+\cdot Cl^-$. Atom labels for **M** are provided in Scheme 1.

spectrum for a 1:1 mixture of **M** + $\mathbf{1}^+\cdot$Cl (Figure S33). The peaks indicated through space interactions between macrocycle proton B and several protons in $\mathbf{1}^+$. A final comparison of spectra for a 1:1 mixture of **M** + $\mathbf{1}^+\cdot BAr_F^-$ (Figure 1c) and 1:1:1 mixture of **M** + $\mathbf{1}^+\cdot BAr_F^-$ + $TBA^+\cdot Cl^-$ (Figure 1d) shows that the presence of the $Cl^-$ promotes binding of $\mathbf{1}^+$ inside **M** (indicated by the upfield changes in chemical shifts for the protons in $\mathbf{1}^+$ and downfield changes in chemical shift for the NH residues and protons B in **M**). Together, this collection of spectral data suggests that the affinity of **M** for $Cl^-$ is enhanced when the countercation ($Q^+$) is changed from $TBA^+$ to $\mathbf{1}^+$ because **M** binds $\mathbf{1}^+\cdot Cl^-$ as an ion pair with $\mathbf{1}^+$ stabilized inside the cavity of **M**.

This conclusion was confirmed and quantified by conducting a series of separate NMR titration experiments that added different salts $Q^+\cdot Cl^-$ to a solution of **M** in $CDCl_3$ and measured the $Cl^-$ affinity ($K_a$). As a starting point, we added aliquots of $TBA^+\cdot Cl^-$ to **M** and generated titration isotherms by plotting the changes in chemical shift for the macrocycle peaks. As shown by the data in Figure S38, there was a large downfield change in NH chemical shift indicating hydrogen bonding between the $Cl^-$ and the amide NH residues in **M**. The titration isotherms were found to fit nicely to a 1:1 binding model, and a weak $K_a$ of 50 $M^{-1}$ was determined (Figure S39). The next NMR titration experiment added $\mathbf{1}^+\cdot Cl^-$ to a solution of **M** (Figure S40). Nonlinear fitting of the titration isotherm (Figure S41) and an independent Job's plot (Figure S36) both indicated a 1:1 binding stoichiometry and a $K_a$ of 890 $M^{-1}$. In other words, substituting $TBA^+$ for $\mathbf{1}^+$ increased $Cl^-$ affinity for **M** by 19-fold.[30]

The changes in NMR chemical shifts for binding of **M** by $\mathbf{1}^+\cdot$Cl indicated that the acetyl-bearing arm of $\mathbf{1}^+$ penetrated deep inside the cavity of **M**. Computer-based molecular modeling of the complex suggested the supramolecular complex $\mathbf{1}^+\cdot Cl^-$@**M** that is shown in Figure 3a with the carbonyl oxygen of $\mathbf{1}^+$ hydrogen bonded with the second pair of macrocycle NH residues. To quantify the relative importance of this internal hydrogen bonding between **M** and $\mathbf{1}^+$, we measured $K_a$ for binding of two homologues of $\mathbf{1}^+\cdot Cl^-$ that have a similar shape as $\mathbf{1}^+$ but attenuated hydrogen-bonding capacity. The two homologues were $\mathbf{2}^+\cdot Cl^-$ and $\mathbf{3}^+\cdot Cl^-$, and the measured $K_a$ values of 950 and 930 $M^{-1}$ (Figures S44–S47), respectively, were essentially the same. In each case, there was a large complexation-induced downfield change in NMR chemical shift for macrocycle proton B and upfield changes in chemical

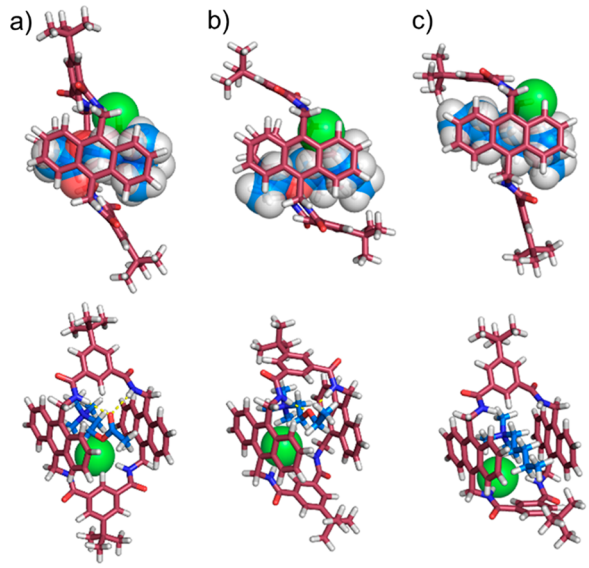


**Figure 3.** Energy-minimized structure (semiempirical, PM7) of (a) $\mathbf{1}^+\cdot Cl^-$@**M**, (b) $\mathbf{2}^+\cdot Cl^-$@**M**, and (c) $\mathbf{3}^+\cdot Cl^-$@**M**.

shift for several of the protons on the longest arm of the $Q^+$ cation (Figures S68–S69). Both NMR effects are consistent with deep penetration of $Q^+$ inside the cavity of **M**.

A computer-based molecular model of $\mathbf{2}^+\cdot Cl^-$@**M** (Figure 3b) indicated hydrogen bonding between the ether oxygen in $\mathbf{2}^+$ and the second pair of macrocycle NH residues. In the case of $\mathbf{3}^+\cdot Cl^-$@**M** there is no heteroatom within $\mathbf{3}^+$ that is available for hydrogen bonding with the macrocycle NH residues, but there is the possibility of multiple CH–$\pi$ interactions between the pentyl arm of $\mathbf{3}^+$ and the aromatic surfaces that line the cavity of **M** (Figure 3c).[31]

The idea that $Q^+$ could interact with the aromatic sidewalls of **M** led us to consider $Q^+$ structures that could form $\pi$–$\pi$ stacking interactions. Thus, we prepared chloride salts of the eight benzylic trimethylammonium cations $\mathbf{4}^+$–$\mathbf{11}^+$ by reacting the parent benzyl bromide with trimethylamine (Scheme 2).

**Scheme 2. Synthesis of $\mathbf{4}^+\cdot Cl^-$–$\mathbf{11}^+\cdot Cl^-$**

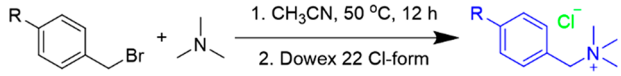


The only difference between the cationic structures was the identity of the para substituent, R, on the benzylic arm, which ranged from strongly electron-donating *p*-OMe to strongly electron-withdrawing *p*-$NO_2$. Association of each salt with **M** was characterized using $^1$H NMR spectroscopy. In each case, there was an upfield, complexation-induced change in chemical shift for the benzylic protons on $Q^+$ indicating a location deep inside the macrocycle cavity and stacked against the anthracene sidewalls of **M** (Figures 4, S48–S63, and S68–S75). In the case of $\mathbf{8}^+\cdot Cl^-$ complexation by **M**, a Job's plot confirmed 1:1 binding stoichiometry (Figure S37) and a ROESY spectrum of the complex indicated through-space interactions between macrocycle proton B and several protons in $\mathbf{8}^+$ (Figure S34).

Listed in Table 1 are $K_a$ values for binding of $\mathbf{4}^+\cdot Cl^-$–$\mathbf{11}^+\cdot Cl^-$ by **M** as determined by the NMR titration experiments. To better understand the interaction of $Q^+$ with the anthracene sidewalls of **M**, the logarithm of the relative association



DOI: 10.1021/acs.joc.8b03197
J. Org. Chem. 2019, 84, 2808–2816

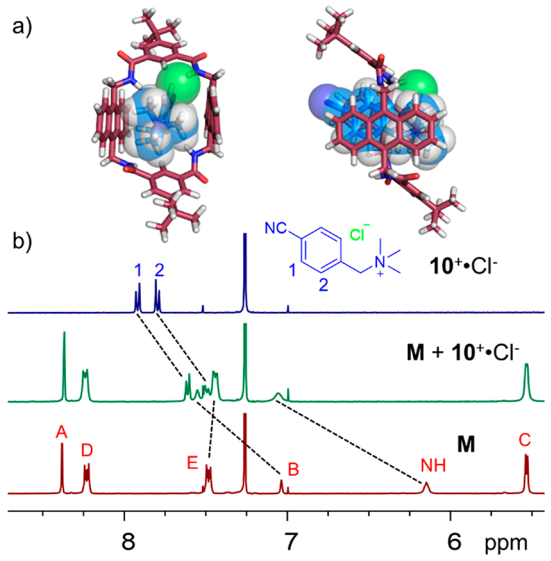


**Figure 4.** (a) Energy-minimized structure (semiempirical, PM7) of $10^+ \cdot Cl^-$@**M**. (b) Partial $^1$H NMR spectra (500 MHz, $CDCl_3$, 1 mM, 25 °C) of $10^+ \cdot Cl^-$ (top) and **M** (bottom) and their equimolar mixture (middle). Atom labels for **M** are provided in Scheme 1.

**Table 1. Association Constants ($K_a$) for Guest Binding to M in $CDCl_3$ at 25 °C**[a]

| guest | $K_a$ ($10^3$ $M^{-1}$) | $\Delta G$ (kcal·$mol^{-1}$) |
|---|---|---|
| $TBA^+ \cdot Cl^-$ | 0.05 ± 0.01 | −2.29 ± 0.03 |
| $1^+ \cdot Cl^-$ | 0.89 ± 0.03 | −4.03 ± 0.02 |
| $2^+ \cdot Cl^-$ | 0.95 ± 0.06 | −4.06 ± 0.04 |
| $3^+ \cdot Cl^-$ | 0.93 ± 0.02 | −4.05 ± 0.02 |
| $4^+ \cdot Cl^-$ | 2.10 ± 0.07 | −4.54 ± 0.02 |
| $5^+ \cdot Cl^-$ | 1.78 ± 0.13 | −4.44 ± 0.04 |
| $6^+ \cdot Cl^-$ | 2.95 ± 0.15 | −4.74 ± 0.03 |
| $7^+ \cdot Cl^-$ | 5.32 ± 0.69 | −5.09 ± 0.07 |
| $8^+ \cdot Cl^-$ | 3.66 ± 0.25 | −4.87 ± 0.03 |
| $9^+ \cdot Cl^-$ | 2.92 ± 0.18 | −4.73 ± 0.04 |
| $10^+ \cdot Cl^-$ | 7.86 ± 1.82 | −5.32 ± 0.12 |
| $11^+ \cdot Cl^-$ | 6.02 ± 0.42 | −5.16 ± 0.04 |

[a]Determined by $^1$H NMR titration.

constant ($K_R/K_H$) for $4^+ \cdot Cl^- - 11^+ \cdot Cl^-$ was plotted against the Hammett para-substituent parameter $\sigma_p$ (Figure 5).[32] The plot exhibits a rough linear trend (slope of +0.52 ± 0.15) with affinity for **M** usually increased by having electron withdrawing para-substituents on $Q^+$. There are likely multiple factors controlling the observed substituent effects on binding energy, including (a) strength of the ion-pair interactions between $Q^+$ and $Cl^-$, (b) aromatic stacking interactions between $Q^+$ and **M**, (c) benzylic CH−$\pi$ interactions between $Q^+$ and **M**, and (d) steric repulsion in the case of the relatively large *p*-$COOCH_3$ substituent. The highest affinity for the series was observed with $10^+ \cdot Cl^-$, which contained a *p*-CN substituent, and the measured value of $K_a$ = 7.9 × $10^3$ $M^{-1}$ is 160-fold higher than the $K_a$ for binding of $TBA^+ \cdot Cl^-$ by **M**.

**Templated Macrocyclization Synthesis of M.** The synthesis of macrocycle **M** and its close analogues can be achieved by reacting 9,10-bis(aminomethyl)anthracene (**12**) with the corresponding 1,3-isophthaloyl derivative (**13**). Under these conditions, a low yield (<20%) of the [2 + 2] macrocycle is obtained along with linear oligomers and higher order macrocycles as impurities. A classic synthetic approach to

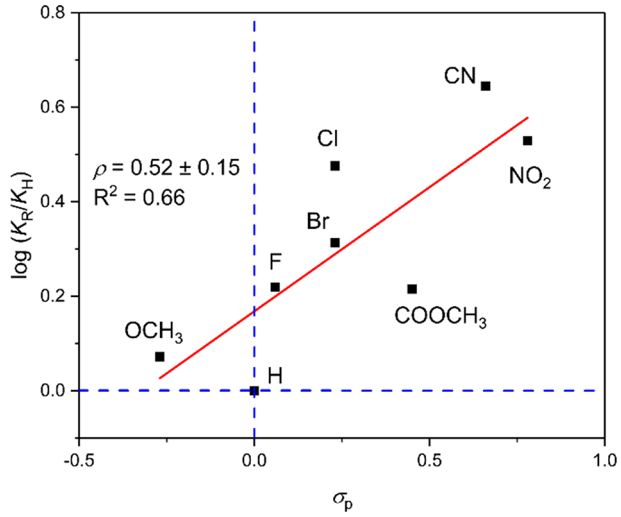


**Figure 5.** Plot of relative association constants $\log(K_R/K_H)$ and Hammett para-substituent parameter $\sigma_p$. The red line is a linear best fit of the points.

improving the yield of a macrocyclization process is to conduct the reaction in the presence of an inert template molecule that has affinity for the reactive intemediate(s) produced during the reaction and selectively promotes the desired cyclization step.[33−37]

Having identified $10^+ \cdot Cl^-$ as a high-affinity guest for **M**, we investigated if it could be used as a macrocyclization template. As summarized in Scheme 3, a series of comparative macrocyclization reactions was conducted on the 100 mg scale, in the absence or presence of $10^+ \cdot Cl^-$. After the

**Scheme 3. (a) Macrocyclization Reactions Conducted in the Presence and Absence of 1 Molar Equiv of $10^+ \cdot Cl^-$. (b) Intramolecular Cyclization of the Penultimate Reactive Intermediate Promoted by Noncovalent Interactions with $10^+ \cdot Cl^-$ as a Reaction Template**

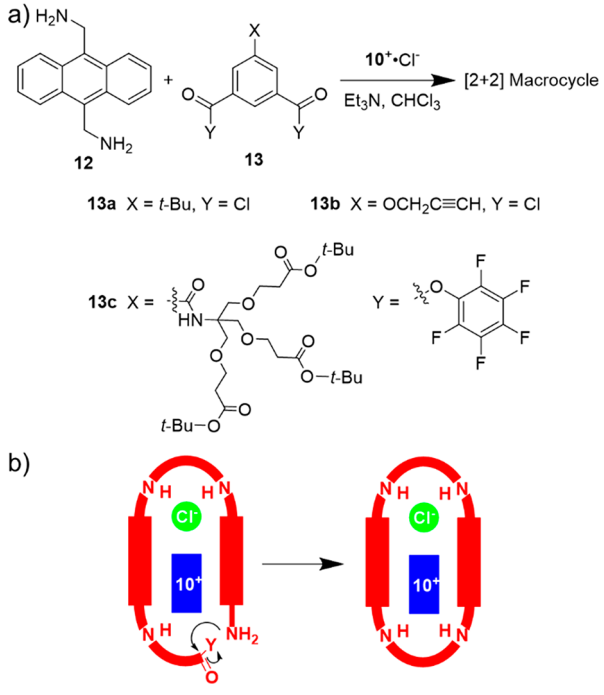




DOI: 10.1021/acs.joc.8b03197
J. Org. Chem. 2019, 84, 2808−2816

completion of each reaction, the solvent was removed and the crude product determined by integration of appropriate $^1$H NMR peaks. A comparison of entries 1 and 2 in Table 2 shows

**Table 2. Crude Yields of [2 + 2] Macrocycle Product**

| entry | Reagent | $10^+\cdot Cl^-$ template | crude yield (%) |
|---|---|---|---|
| 1 | **13a** | no | 19 |
| 2 | **13a** | yes | 50 |
| 3 | **13b** | yes | 27 |
| 4 | **13c** | yes | 43 |

that the presence of $10^+\cdot Cl^-$ in the reaction increased the crude yield of **M** from 19% to 50%. The ion-pair template was completely removed by extracting the crude product with methanol, and after subsequent selective extraction steps, pure **M** was obtained in 46% isolated yield without requiring column chromatography. Entries 3 and 4 in Table 2 show that the same ion-pair template ($10^+\cdot Cl^-$) could be used to improve the synthesis yields of two structural analogues of **M** that are needed for our ongoing research efforts.[38] In Scheme 3b is a mechanistic picture of the template-promoted macrocyclization step. Attractive noncolvalent interactions between the penultimate reactive intermediate and the $10^+\cdot Cl^-$ ion pair increase the likelihood of an intramolecular cyclization over competing intermolecular reactions.

**Rotaxane Synthesis.** The success with a templated macrocyclization prompted us to try a threaded "capping" reaction[27,39,40] that traps a dumbbell-shaped organic cation inside **M** and produces a mechanically interlocked rotaxane, an approach that is conceptually different from other literature methods of creating rotaxanes using the anion component of an ion pair as a template.[41] As shown in Scheme 4, the benzylic ion pair $16^+\cdot Cl^-$, whose structure includes a terminal alkyne group, was prepared in straightforward fashion and then subjected to a biphasic azide/alkyne cycloaddition reaction in the presence of **M** to produce the rotaxanated ion-pair $\mathbf{M}\supset\mathbf{17}^+\cdot Cl^-$ in low yield.[42]

The structure of $\mathbf{M}\supset\mathbf{17}^+\cdot Cl^-$ was characterized by a combination of mass spectrometry (Figure S30), $^1$H NMR, and COSY (Figures S29 and S35). Figure 6 shows a comparison of partial $^1$H NMR spectra for the rotaxane and the free components in $CD_3OD$. As expected, rotaxane formation induced a downfield change in chemical shift for the macrocycle protons B, whereas the axle phenylene protons 6 and 7 moved significantly upfield. Because of the unsymmetric axle, the macrocycle protons C−E are not equivalent, and there is a pair of peaks for each set of protons. The macrocycle protons A and B are single peaks indicating signal averaging due to rapid pirouetting of the macrocycle around the axle, which is consistent with the molecular dynamics exhibited by a structurally related rotaxane with the same macrocycle **M** but different axle component.[43]

## CONCLUSIONS

The ability of tetralactam macrocyclic receptor **M** to bind $Cl^-$ in weakly polar chloroform solution depends strongly on the shape of the counter quaternary ammonium cation ($Q^+$). Values of $K_a$ were enhanced (i.e., positive binding cooperativity) when the shape and functionality of the quaternary ammonium cation allowed it to penetrate the macrocycle cavity and engage in attractive noncovalent interactions with the macrocycle's NH resides and aromatic sidewalls. A

**Scheme 4. Synthesis of Rotaxane Ion Pair $\mathbf{M}\supset\mathbf{17}^+\cdot Cl^-$**

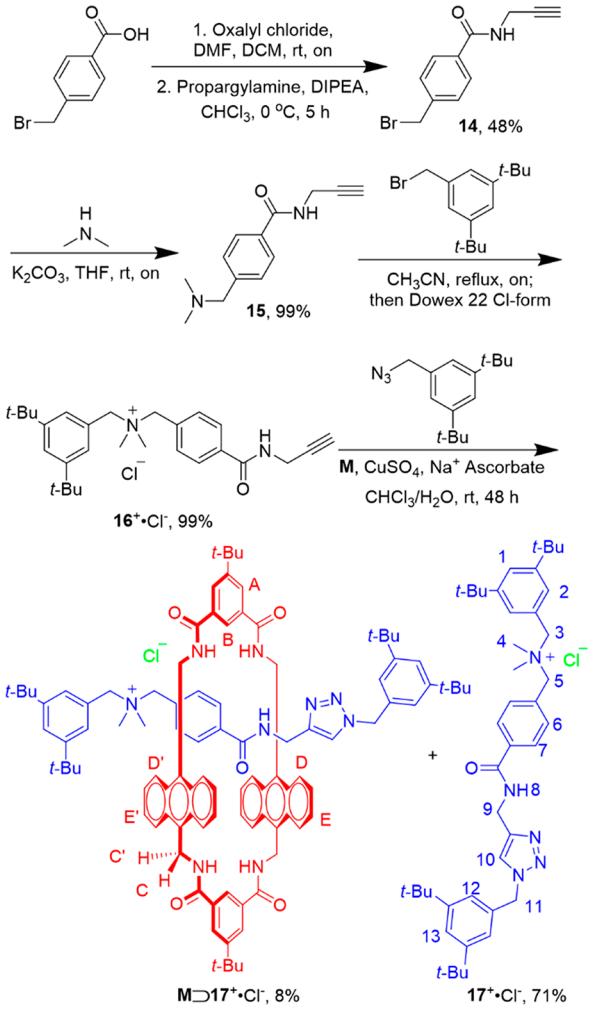


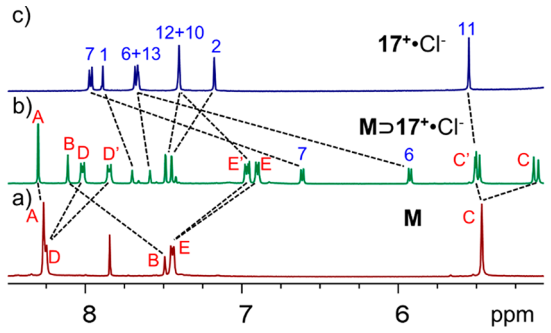


**Figure 6.** Partial $^1$H NMR spectra (500 MHz, 2 mM, 25 °C) of (a) **M** in $CD_3OD/CDCl_3$ (9:1, v/v), (b) rotaxane $\mathbf{M}\supset\mathbf{17}^+\cdot Cl^-$ in $CD_3OD$, and (c) free axle $\mathbf{17}^+\cdot Cl^-$ in $CD_3OD$. Atom labels are provided in Scheme 4. Note that the NH signals are absent due to exchange with the $CD_3OD$ solvent.

structure/affinity study revealed enhanced macrocycle affinity when $Q^+$ was a benzylic trimethylammonium cation with an electron-withdrawing *p*-CN substituent on the benzyl ring (i.e., $10^+$) which favors aromatic stacking and CH−$\pi$ interactions between $Q^+$ and **M**. The yields of macrocyclization reactions that make **M** or structurally related derivatives were increased substantially when $10^+\cdot Cl^-$ was present as a stoichiometric macrocyclization template. A new type of rotaxanated ion pair,



DOI: 10.1021/acs.joc.8b03197
J. Org. Chem. 2019, 84, 2808−2816

**M⊃17**$^{+}$·Cl$^{-}$, was prepared by "capping" the end of a self-assembled complex comprised of **M** threaded by a reactive benzylic quaternary ammonium cation (i.e., **16**$^{+}$). This new synthetic method provides access to novel rotaxanated ion pairs that are likely to exhibit interesting behavior as a anion sensors, molecular shuttles, or transport molecules.[44−46]

## EXPERIMENTAL SECTION

**General Methods.** $^{1}$H, $^{13}$C, COSY, and ROESY NMR spectrum were recorded on a 500 or 400 MHz NMR spectrometer. Chemical shifts are presented in ppm and referenced by residual solvent peak. High-resolution mass spectrometry (HRMS) was performed using a time-of-flight (TOF) analyzer with electron-spray ionization (ESI).

**Synthetic Procedures.** *2-Acetyloxy-N,N,N-trimethylethanaminium Tetrakis[3,5-bis(trifluoromethyl)phenyl]boron (**1**$^{+}$·BAr$_F^-$).* Compound **1**$^{+}$·Cl$^{-}$ (100 mg, 0.550 mmol) and sodium tetrakis[3,5-bis(trifluoromethyl)phenyl]borate (976 mg, 1.10 mmol) were dissolved in methanol (10 mL). The mixture was stirred at room temperature for 4 h. Solvent was removed under reduced pressure, and the residue was suspended in water (20 mL). The mixture was extracted with dichloromethane (3 × 20 mL). The organic layers were combined and washed with water (60 mL). Solvent was removed to afford the product as a light yellow powder (500 mg, 90%). Mp = 115−118 °C. $^{1}$H NMR (400 MHz, $CDCl_3$, 25 °C) $\delta$ (ppm) 7.70−7.69 (m, 8H), 7.56 (s, 4H), 4.40−4.36 (m, 2H), 3.34−3.32 (m, 2H), 2.90 (s, 9H), 2.10 (s, 3H). HRMS (ESI-TOF) $m/z$: [M]$^{+}$ calcd for $C_7H_{16}NO_2^{+}$ 146.1176, found 146.1176, [M]$^{-}$ calcd for $C_{32}H_{12}BF_{24}^{-}$ 863.0645, found 863.0654.

*General Synthetic Procedure for Compounds **2**$^{+}$·Cl$^{-}$ and **3**$^{+}$·Cl$^{-}$.* 2-Bromoethyl ethyl ether or 1-bromopentane (1 equiv, 887 $\mu$M), trimethylamine (2 M in MeCN, 3 equiv, 1.33 mL, 2.66 mM), and MeCN (10 mL) were added to a round-bottom flask equipped with a stir bar. The mixture was stirred at 90 °C for 8 h. After the mixture was cooled to room temperature, diethyl ether (20 mL) was added to form a white precipitate which was collected by filtration and further washed with diethyl ether/dichloromethane (1:1, v/v) in an ultrasonic bath. The solid was dried to obtain the corresponding bromide salt. Chloride-exchange resin (Dowex 22 chloride form) (12 g) was washed with deionized water and loaded on to a column which was eluted first with 5% HCl (200 mL) and then deionized water until the pH of the eluted solution was neutral. The solid bromide salt was dissolved in MeCN and loaded to the column of chloride-exchange resin. The column was eluted with MeCN (200 mL) and the eluted solvent removed to obtain the desired chloride salt. The presence of Cl$^{-}$ was confirmed and quantified by $AgNO_3$ titration.

*2-Ethoxy-N,N,N-trimethylethanaminium Chloride (**2**$^{+}$·Cl)$^{-}$.* White solid (140 mg, 94%). Mp = 115−120 °C. $^{1}$H NMR (400 MHz, $CDCl_3$, 25 °C) $\delta$ (ppm): 4.03−3.96 (m, 2H), 3.95−3.89 (m, 2H), 3.56 (q, $J$ = 7.0 Hz, 2H), 3.46 (s, 9H), 1.22 (t, $J$ = 7.0 Hz, 3H). $^{13}$C{$^{1}$H} NMR (125 MHz, $CDCl_3$, 25 °C) $\delta$ (ppm): 67.0, 65.6, 64.5, 54.5, 15.0. HRMS (ESI-TOF) $m/z$: [M]$^{+}$ calcd for $C_7H_{18}NO^{+}$ 132.1383, found 132.1371.

*N,N,N-Trimethyl-1-pentanaminium Chloride (**3**$^{+}$·Cl$^{-}$).* White solid (146 mg, 99%). Mp = 145−148 °C. $^{1}$H NMR (400 MHz, $CDCl_3$, 25 °C) $\delta$ (ppm): 3.61−3.51 (m, 2H), 3.46 (s, 9H), 1.85−1.32 (m, 2H), 1.57 (s, 4H), 1.05−0.86 (m, 3H). $^{13}$C{$^{1}$H} NMR (125 MHz, $CDCl_3$, 25 °C) $\delta$ (ppm): 67.0, 53.4, 28.3, 23.0, 22.4, 13.9. HRMS (ESI-TOF) $m/z$: [M]$^{+}$ calcd for $C_8H_{20}N^{+}$ 130.1590, found 130.1578.

*General Synthetic Procedure for Compounds **4**$^{+}$·Cl$^{-}$, **5**$^{+}$·Cl$^{-}$, **6**$^{+}$·Cl$^{-}$, **7**$^{+}$·Cl$^{-}$, **8**$^{+}$·Cl$^{-}$, **9**$^{+}$·Cl$^{-}$, **10**$^{+}$·Cl$^{-}$, and **11**$^{+}$·Cl$^{-}$.* The benzyl bromide precursor (100 mg), $CH_3CN$ (3 mL), and trimethylamine (2 M in MeCN, 2 mL) were added to a 20 mL vial. The mixture was stirred at 50 °C for 12 h. After the mixture was cooled to room temperature, diethyl ether (20 mL) was added to give the bromide salt product as a precipitate. The white precipitate was collected by filtration and further washed with diethyl ether/dichloromethane (1:1, v/v) in an ultrasonic bath. The solid bromide salt was dried and converted to the desired chloride salt using the ion-exchange procedure described above.

*4-Methoxy-N,N,N-trimethylbenzenemethanaminium Chloride (**4**$^{+}$·Cl$^{-}$).* White solid (100 mg, 92%). Mp = 35−38 °C. $^{1}$H NMR (500 MHz, $CDCl_3$, 25 °C) $\delta$ (ppm): 7.51 (d, $J$ = 8.7 Hz, 2H), 6.85 (d, $J$ = 8.7 Hz, 2H), 4.89 (s, 2H), 3.75 (s, 3H), 3.30 (s, 9H).$^{13}$C{$^{1}$H} NMR (125 MHz, $CDCl_3$, 25 °C) $\delta$ (ppm): 161.3, 134.5, 119.6, 114.5, 68.6, 55.4, 52.3. HRMS (ESI-TOF) $m/z$: [M]$^{+}$ calcd for $C_{11}H_{18}NO^{+}$ 180.1383, found 180.1375.

*N,N,N-Trimethylbenzenemethanaminium Chloride (**5**$^{+}$·Cl$^{-}$).* White solid (108 mg, 99%). Mp = 205−208 °C. $^{1}$H NMR (500 MHz, $CDCl_3$, 25 °C) $\delta$ (ppm): 7.64 (d, $J$ = 8.5 Hz, 2H), 7.49−7.44 (m, 1H), 7.44−7.39 (m, 2H), 5.02 (s, 2H), 3.40 (s, 9H). $^{13}$C{$^{1}$H} NMR (125 MHz, $CDCl_3$, 25 °C) $\delta$ (ppm): 133.2, 130.9, 129.3, 127.7, 69.1, 52.8. HRMS (ESI-TOF) $m/z$: [M]$^{+}$ calcd for $C_{10}H_{16}N^{+}$ 150.1277, found 150.1260.

*4-Fluoro-N,N,N-trimethylbenzenemethanaminium Chloride (**6**$^{+}$·Cl$^{-}$).* White solid (106 mg, 99%). Mp = 206−209 °C. $^{1}$H NMR (500 MHz, $CDCl_3$, 25 °C) $\delta$ (ppm): 7.69 (dd, $J$ = 8.6, 5.3 Hz, 2H), 7.14 (dd, $J$ = 8.6 Hz, 2H), 5.08 (s, 2H), 3.37 (s, 9H). $^{13}$C{$^{1}$H} NMR (125 MHz, $CDCl_3$, 25 °C) $\delta$ (ppm): 135.4, 135.3, 116.7, 116.5, 68.1, 52.7. HRMS (ESI-TOF) $m/z$: [M]$^{+}$ calcd for $C_{10}H_{15}FN^{+}$ 168.1183, found 168.1163.

*4-Chloro-N,N,N-trimethylbenzenemethanaminium Chloride (**7**$^{+}$·Cl$^{-}$).* White solid (103 mg, 96%). Mp = 184−187 °C. $^{1}$H NMR (500 MHz, $CDCl_3$, 25 °C) $\delta$ (ppm): 7.65 (d, $J$ = 8.4 Hz, 2H), 7.40 (d, $J$ = 8.4 Hz, 2H), 5.12 (s, 2H), 3.39 (s, 9H). $^{13}$C{$^{1}$H} NMR (125 MHz, $CDCl_3$, 25 °C) $\delta$ (ppm): 137.4, 134.6, 129.6, 126.2, 67.9, 52.8. HRMS (ESI-TOF) $m/z$: [M]$^{+}$ calcd for $C_{10}H_{15}ClN^{+}$ 184.0888, found 184.0865.

*4-Bromo-N,N,N-trimethylbenzenemethanaminium Chloride (**8**$^{+}$·Cl$^{-}$).* White solid (105 mg, 99%). Mp = 170−172 °C. $^{1}$H NMR (500 MHz, $CDCl_3$, 25 °C) $\delta$ (ppm): 7.57 (m, 4H), 5.12 (s, 2H), 3.39 (s, 9H). $^{13}$C{$^{1}$H} NMR (125 MHz, $CDCl_3$, 25 °C) $\delta$ (ppm): 134.8, 132.7, 126.7, 125.9, 68.0, 52.8. HRMS (ESI-TOF) $m/z$: [M]$^{+}$ calcd for $C_{10}H_{15}BrN^{+}$ 228.0382, found 228.0355.

*4-(Methoxycarbonyl)-N,N,N-trimethylbenzenemethanaminium Chloride (**9**$^{+}$·Cl$^{-}$).* White solid (100 mg, 91%). Mp = 175−180 °C. $^{1}$H NMR (500 MHz, $CDCl_3$, 25 °C) $\delta$ (ppm): 8.06 (d, $J$ = 8.2 Hz, 2H), 7.79 (d, $J$ = 8.2 Hz, 2H), 5.23 (s, 2H), 3.93 (s, 3H), 3.43 (s, 9H). $^{13}$C{$^{1}$H} NMR (125 MHz, $CDCl_3$, 25 °C) $\delta$ (ppm): 166.2, 133.4, 132.5, 132.3, 130.3, 68.0, 53.0, 52.7. HRMS (ESI-TOF) $m/z$: [M]$^{+}$ calcd for $C_{12}H_{18}NO_2^{+}$ 208.1332, found 208.1306.

*4-Cyano-N,N,N-trimethylbenzenemethanaminium Chloride (**10**$^{+}$·Cl$^{-}$).* White solid (107 mg, 99%). Mp = 228−230 °C. $^{1}$H NMR (500 MHz, $CDCl_3$, 25 °C) $\delta$ (ppm): 7.93 (d, $J$ = 8.2 Hz, 2H), 7.78 (d, $J$ = 8.2 Hz, 2H), 5.36 (s, 2H), 3.44 (s, 9H). $^{13}$C{$^{1}$H} NMR (125 MHz, DMSO-$d_6$, 25 °C) $\delta$ (ppm): 133.84, 133.72, 132.73, 118.34, 112.96, 66.33, 51.91. HRMS (ESI-TOF) $m/z$: [M]$^{+}$ calcd for $C_{11}H_{15}N_2^{+}$ 175.1230, found 175.1203.

*4-Nitro-N,N,N-trimethylbenzenemethanaminium Chloride (**11**$^{+}$·Cl$^{-}$).* White solid (106 mg, 99%). Mp = 170−172 °C. $^{1}$H NMR (500 MHz, $CDCl_3$, 25 °C) $\delta$ (ppm): 8.33 (d, $J$ = 8.6 Hz, 2H), 8.00 (d, $J$ = 8.6 Hz, 2H), 5.36 (s, 2H), 3.41 (s, 9H).). $^{13}$C{$^{1}$H} NMR (125 MHz, DMSO-$d_6$, 25 °C) $\delta$ (ppm): 148.6, 135.5, 134.4, 123.8, 66.0, 52.0. HRMS (ESI-TOF) $m/z$: [M]$^{+}$ calcd for $C_{10}H_{15}N_2O_2^{+}$ 195.1128, found 195.1105.

*General Templated Synthesis of [2 + 2] Macrocycle.* A member of the compound class **13** (0.320 mmol) was dissolved in a solution containing anhydrous chloroform (10 mL). Compound 9,10-anthracenedimethanamine **12** (82.9 mg, 0.320 mmol) was dissolved in a solution of anhydrous chloroform (10 mL) with trimethylamine (0.5 mL). Both aliquots were added over 12 h by dual syringe pump into a stirring solution of **10**$^{+}$·Cl$^{-}$ (67.2 mg, 0.320 mmol) in anhydrous chloroform (20 mL). The mixture was stirred at room temperature for an additional 24 h after injection. The mixture was washed with 5% HCl (50 mL), water (50 mL), and brine (50 mL) and dried over $Na_2SO_4$. The solvent was evaporated, and the crude yield was measured by integration of $^{1}$H NMR peaks using pyrazine as an added internal standard. In the specific case of reactant **13a**, the



DOI: 10.1021/acs.joc.8b03197
J. Org. Chem. 2019, 84, 2808−2816

crude product containing **M** was suspended in MeOH (80 mL) and sonicated for 2 h at room temperature to remove the $\mathbf{10}^+\cdot Cl^-$ template. The mixture was filtered, and the solid was suspended in $CHCl_3$ (10 mL) and filtered through a Celite pad. Hexane (100 mL) was added to the filtrate to precipitate **M**, and the mixture was cooled in a −30 °C freezer for 30 min. The solid was collected by filtration, washed with acetone (10 mL), and dried to afford **M** as a yellow solid (63 mg, 46% isolated yield) whose structure and high purity were confirmed by $^1$H NMR (Figure S22).

*4-(Bromomethyl)-N-2-propyn-1-ylbenzamide (**14**).* Compound 4-(bromomethyl)benzoic acid (1.00 g, 4.65 mmol) was suspended in DCM (20 mL), and oxalyl chloride (2.36 g, 18.6 mmol) was added to the suspension followed by two drops of *N*,*N*-dimethylformamide. The mixture was stirred under argon atmosphere until the solid was completely dissolved. The solvent was removed, and the residue was dissolved in dry $CHCl_3$ (50 mL). After the solution was cooled with an ice bath, a solution of propargylamine (0.298 mL, 4.65 mmol) and diisopropyl ethylamine (3.84 mL, 23.3 mmol) in 20 mL of dry $CHCl_3$ was added dropwise. The mixture was stirred, with ice bath cooling, for 5 h after addition. The solvent was removed and the residue purified by column chromatography ($SiO_2$, 20−60% ethyl acetate in hexane) to afford the product as a yellow solid (560 mg, 48%). Mp = 131−135 °C. $^1$H NMR (500 MHz, $CDCl_3$, 25 °C) $\delta$ (ppm): 7.78 (d, $J$ = 8.2 Hz, 2H), 7.46 (d, $J$ = 8.2 Hz, 2H), 6.38 (br s, 1H), 4.61 (s, 2H), 4.25 (dd, $J$ = 5.2, 2.6 Hz, 2H), 2.29 (t, $J$ = 2.6 Hz, 1H). $^{13}$C{$^1$H} NMR (125 MHz, $CDCl_3$, 25 °C) $\delta$ (ppm): 166.7, 141.4, 129.5, 129.0, 127.7, 79.6, 72.2, 45.5, 30.1. HRMS (ESI-TOF) $m/z$: $[M + H]^+$calcd for $C_{11}H_{11}BrNO^+$ 252.0019, found 251.9994.

*4-[(Dimethylamino)methyl]-N-2-propyn-1-yl-benzamide (**15**).* A mixture of compound **14** (300 mg, 1.19 mmol), dimethylamine (2 M in THF, 5.95 mL, 11.9 mmol), and $K_2CO_3$ (493 mg, 3.57 mmol) in dry THF (10 mL) was stirred overnight. Water (50 mL) was added, and the mixture was extracted with $CHCl_3$ (3 × 30 mL). The organic layers were combined, dried over $Na_2SO_4$, then evaporated to afford the product as a yellow solid (257 mg, 99%). Mp = 65−68 °C. $^1$H NMR (500 MHz, $CDCl_3$, 25 °C) $\delta$ (ppm): 7.73 (d, $J$ = 8.2 Hz, 2H), 7.35 (d, $J$ = 8.2 Hz, 2H), 6.61 (t, $J$ = 5.2 Hz, 1H), 4.22 (dd, $J$ = 5.2, 2.5 Hz, 2H), 3.43 (s, 2H), 2.25 (t, $J$ = 2.5 Hz, 1H), 2.21 (s, 3H). $^{13}$C{$^1$H} NMR (125 MHz, $CDCl_3$, 25 °C) $\delta$ (ppm): 167.3, 143.2, 132.7, 129.4, 127.3, 79.8, 72.0, 64.1, 45.6, 29.9. HRMS (ESI-TOF) $m/z$: $[M + H]^+$ calcd for $C_{13}H_{17}N_2O^+$ 217.1335, found 217.1316.

*Compound $\mathbf{16}^+\cdot Cl^-$.* A solution of compound **15** (100 mg, 0.462 mmol) and 3,5-di-*tert*-butylbenzyl bromide (144 mg, 0.509 mmol) in $CH_3CN$ (20 mL) was stirred at 90 °C for 12 h. The resulting mixture was allowed to cool to room temperature, and diethyl ether (20 mL) was added to form a white precipitate. The precipitate was collect by filtration, further washed with diethyl ether in ultrasonic bath, then dried to give the corresponding bromide salt which was converted to the chloride salt using the ion-exchange procedure described above. The desired product was obtained as a yellow solid (210 mg, 99%). Mp = 202−205 °C. $^1$H NMR (500 MHz, $CDCl_3$, 25 °C) $\delta$ (ppm): 9.03 (t, $J$ = 5.5 Hz, 1H), 7.96 (d, $J$ = 7.6 Hz, 2H), 7.71 (d, $J$ = 7.6 Hz, 2H), 7.51 (t, $J$ = 1.8 Hz, 1H), 7.31 (d, $J$ = 1.8 Hz, 2H), 5.27 (s, 2H), 4.80 (s, 2H), 4.22 (dd, $J$ = 5.5, 2.5 Hz, 2H), 3.06 (s, 6H), 2.24 (s, 1H), 1.29 (s, 18H). $^{13}$C{$^1$H} NMR (125 MHz, $CDCl_3$, 25 °C) $\delta$ (ppm): 167.0, 152.3, 136.5, 133.6, 130.9, 128.6, 127.7, 126.4, 124.8, 80.7, 71.1, 68.7, 67.8, 48.5, 35.1, 31.6, 29.7. HRMS (ESI-TOF) $m/z$: $[M]^+$ calcd for $C_{28}H_{39}N_2O^+$ 419.3057, found 419.3054.

*Rotaxane $\mathbf{M}\supset\mathbf{17}^+\cdot Cl^-$ and Free Axle $\mathbf{17}^+\cdot Cl^-$.* The ion-pair $\mathbf{16}^+\cdot Cl^-$ (10.0 mg, 22.0 $\mu$mol), 3,5-di-*tert*-butylbenzyl azide (10.8 mg, 44.0 $\mu$mol), and **M** (37.5 mg, 44.0 $\mu$mol) were dissolved in $CHCl_3$ (5 mL) and $H_2O$ (1 mL). $CuSO_4\cdot 5H_2O$ (2.74 mg, 11.0 $\mu$mol) and sodium ascorbate (4.35 mg, 22.0 $\mu$mol) were added, and the mixture was stirred at room temperature for 48 h. The solvent was removed, the residue was purified by column chromatography ($SiO_2$, 0−10% MeOH in $CHCl_3$) followed by Dowex 22 column, and the crude product was washed with diethyl ether/hexane (1:1, v/v) to afford $\mathbf{M}\supset\mathbf{17}^+\cdot Cl^-$ and $\mathbf{17}^+\cdot Cl^-$.

*Rotaxane $\mathbf{M}\supset\mathbf{17}^+\cdot Cl^-$.* Yellow solid (2.50 mg, 8%). $^1$H NMR (500 MHz, $CD_3OD$, 25 °C) $\delta$ (ppm): 8.30 (d, $J$ = 1.5 Hz, 4H), 8.11 (t, $J$ = 1.5 Hz, 2H), 8.02 (dd, $J$ = 6.9, 3.3 Hz, 4H), 7.85 (dd, $J$ = 6.9, 3.3 Hz, 4H), 7.70 (t, $J$ = 1.8 Hz, 1H), 7.59 (t, $J$ = 1.8 Hz, 1H), 7.49 (d, $J$ = 1.8 Hz, 2H), 7.45 (d, $J$ = 1.8 Hz, 2H), 6.98−6.95 (m, 5H), 6.90 (dd, $J$ = 6.9, 3.3 Hz, 4H), 6.61 (d, $J$ = 8.0 Hz, 2H), 5.93 (d, $J$ = 8.0 Hz, 2H), 5.51−5.48 (m, 6H), 5.12 (d, $J$ = 14.9 Hz, 4H), 4.43 (s, 2H), 4.32 (s, 2H), 3.63 (s, 2H), 2.74 (s, 6H), 1.47 (s, 18H), 1.40 (s, 18H), 1.39 (s, 18H). The amount of $\mathbf{17}^+\cdot Cl^-$ is not enough for $^{13}$C NMR measurement. HRMS (ESI-TOF) $m/z$: $[M]^+$ calcd for $C_{99}H_{114}N_9O_5^+$ 1508.8937, found 1508.8963.

*Free Axle $\mathbf{17}^+\cdot Cl^-$.* Purple solid (11.0 mg, 71%). Mp = 145−148 °C. $^1$H NMR (500 MHz, $CDCl_3$, 25 °C) $\delta$ (ppm): 8.19 (br s, 1H), 7.89 (d, $J$ = 7.3 Hz, 2H), 7.70 (m, 3H), 7.54 (s, 1H), 7.40 (s, 1H), 7.32 (d, $J$ = 1.8 Hz, 2H), 7.11 (d, $J$ = 1.9 Hz, 2H), 5.48 (s, 2H), 5.29 (s, 2H), 4.81 (s, 2H), 4.72 (d, $J$ = 5.1 Hz, 2H), 3.09 (s, 6H), 1.32 (s, 18H), 1.28 (s, 18H). $^{13}$C{$^1$H} NMR (125 MHz, $CD_3CN$, 25 °C) $\delta$ (ppm): 166.0, 159.0, 152.2, 151.8, 136.6, 135.5, 133.6, 130.6, 128.0, 127.6, 126.6, 125.0, 122.8, 122.7, 122.6, 69.0, 68.2, 54.1, 49.0, 35.3, 34.8, 34.7, 30.8, 30.7. HRMS (ESI-TOF) $m/z$: $[M]^+$ calcd for $C_{43}H_{62}N_5O^+$ 664.4949, found 664.4972.

**NMR Titration Experiments.** All experiments were conducted at 25 °C, and $CDCl_3$ was used as the solvent (the only exceptions were the stock solutions of $\mathbf{6}^+\cdot Cl^-$, $\mathbf{10}^+\cdot Cl^-$, and $\mathbf{11}^+\cdot Cl^-$ which contained 1% $CD_3CN$). Aliquots from a stock solution containing the appropriate chloride salt were added sequentially to an NMR tube containing the macrocyclic host and a $^1$H NMR spectrum was acquired after each addition. The titration isotherms were fitted to a 1:1 binding model using Thordarson's equation.[47] A standard nonlinear squares method within OriginPro 2018 software was used for determining binding constant ($K_a$). All of the titrations were independently duplicated, and a representative titration isotherm for each experiment is provided in the Supporting Information.

**Molecular Modeling.** The starting coordinates of **M** for computer modeling were obtained from the X-ray crystal structures.[48] In each case, an ion-pair guest was added to the cavity, and then the host−guest complex was optimized by the semiempirical method at the PM7 level using the MOPAC program.[49]

## ■ ASSOCIATED CONTENT

### Supporting Information

The Supporting Information is available free of charge on the ACS Publications website at DOI: 10.1021/acs.joc.8b03197.

Spectra for all new compounds, titration data, NMR spectra for complexes and rotaxane, and molecular modeling (PDF)

## ■ AUTHOR INFORMATION


### Corresponding Author

*E-mail: smith.115@nd.edu.

### ORCID

Dong-Hao Li: 0000-0003-2556-1624

Bradley D. Smith: 0000-0003-4120-3210


### Notes

The authors declare no competing financial interest.

## ■ ACKNOWLEDGMENTS

This work was supported by grants from the NSF (CHE1708240). We thank Dr. Evgenii Kovrigin (University of Notre Dame) for help with NMR experiments.

## ■ REFERENCES

(1) Scheerder, J.; vanDuynhoven, J. P. M.; Engbersen, J. F. J.; Reinhoudt, D. N. Solubilization of Nax Salts in Chloroform by Bifunctional Receptors. *Angew. Chem., Int. Ed. Engl.* **1996**, *35*, 1090−1093.



DOI: 10.1021/acs.joc.8b03197
*J. Org. Chem.* 2019, 84, 2808−2816

(2) Smith, B. D. Ion-Pair Recognition by Ditopic Receptors. In *Macrocyclic Chemistry: Current Trends and Future Perspectives*; Gloe, K., Antonioli, B., Eds.; Kluwer: London, 2005; pp 137−151.
(3) Kim, S. K.; Sessler, J. L. Ion Pair Receptors. *Chem. Soc. Rev.* **2010**, *39*, 3784−3809.
(4) McConnell, A. J.; Beer, P. D. Heteroditopic Receptors for Ion-Pair Recognition. *Angew. Chem., Int. Ed.* **2012**, *51*, 5052−5061.
(5) Barboiu, M.; Meffre, A.; Legrand, Y. M.; Petit, E.; Marin, L.; Pinteala, M.; Lee, A. V.D. Frustrated Ion-Pair Binding by Heteroditopic Macrocyclic Receptors. *Supramol. Chem.* **2014**, *26*, 223−228.
(6) Kim, S. K.; Sessler, J. L. Calix[4]Pyrrole-Based Ion Pair Receptors. *Acc. Chem. Res.* **2014**, *47*, 2525−2536.
(7) Ray, S. K.; Homberg, A.; Vishe, M.; Besnard, C.; Lacour, J. Efficient Synthesis of Ditopic Polyamide Receptors for Cooperative Ion Pair Recognition in Solution and Solid States. *Chem. - Eur. J.* **2018**, *24*, 2944−2951.
(8) Mahadevi, A. S.; Sastry, G. N. Cooperativity In Noncovalent Interactions. *Chem. Rev.* **2016**, *116*, 2775−2825.
(9) Shukla, R.; Kida, T.; Smith, B. D. Effect of Competing Akali Metal Cations on Neutral Host's Anion Binding Ability. *Org. Lett.* **2000**, *2*, 3099−3012.
(10) Roelens, S.; Vacca, A.; Francesconi, O.; Venturi, C. Ion-Pair Binding: Is Binding Both Binding Better? *Chem. - Eur. J.* **2009**, *15*, 8296−8302.
(11) Hua, Y.; Ramabhadran, R. O.; Uduehi, E. O.; Karty, J. A.; Raghavachari, K.; Flood, A. H. Aromatic and Aliphatic CH Hydrogen Bonds Fight for Chloride while Competing Alongside Ion Pairing within Triazolophanes. *Chem. - Eur. J.* **2011**, *17*, 312−321.
(12) Späth, A.; König, B. Molecular Recognition of Organic Ammonium Ions in Solution using Synthetic Receptors. *Beilstein J. Org. Chem.* **2010**, *6*, 36.
(13) Gale, P. A.; Howe, E. N. W.; Wu, X. Anion Receptor Chemistry. *Chem.* **2016**, *1*, 351−422.
(14) Wisner, J. A.; Beer, P. D.; Drew, M. G. B. A Demonstration of Anion Templation and Selectivity in Pseudorotaxane Formation. *Angew. Chem., Int. Ed.* **2001**, *40*, 3606−3609.
(15) Arduini, A.; Giorgi, G.; Pochini, A.; Secchi, A.; Ugozzoli, F. Anion Allosteric Effect in the Recognition of Tetramethylammonium Salts by Calix[4]arene Cone Conformers. *J. Org. Chem.* **2001**, *66*, 8302−8308.
(16) Atwood, J. L.; Szumna, A. Hydrogen Bonds Seal Single-Molecule Capsules. *J. Am. Chem. Soc.* **2002**, *124*, 10646−10647.
(17) Mahoney, J. M.; Davis, J. P.; Beatty, A. M.; Smith, B. D. Molecular Recognition of Alkylammonium Contact Ion-Pairs using a Ditopic Receptor. *J. Org. Chem.* **2003**, *68*, 9819−9820.
(18) Sambrook, M. R.; Beer, P. D.; Wisner, J. A.; Paul, R. L.; Cowley, A. R.; Szemes, F.; Drew, M. G. B. Anion-Templated Assembly of Pseudorotaxanes: Importance of Anion Template, Strength of Ion-Pair Thread Association, and Macrocycle Ring Size. *J. Am. Chem. Soc.* **2005**, *127*, 2292−2302.
(19) Bibal, B. Acetylcholine Receptors in Water. *Supramol. Chem.* **2018**, *30*, 243−254.
(20) Moerkerke, S.; Malytskyi, V.; Marcélis, L.; Wouters, J.; Jabin, I. Selective Recognition of Quaternary Ammonium Ions and Zwitterions by using a Biomimetic Bis-Calix[6]Arene-Based Receptor. *Org. Biomol. Chem.* **2017**, *15*, 8967−8974.
(21) Cametti, M.; Dalla Cort, A.; Mandolini, L. Substituent Effects in Cation-$\pi$ Interactions. Recognition of Tetramethylammonium Chloride by Uranyl-Salophen Receptors. *Chem. Sci.* **2012**, *3*, 2119−2122.
(22) Amato, M. E.; Ballistreri, F. P.; D'Agata, S.; Pappalardo, A.; Tomaselli, G. A.; Toscano, R. M.; Sfrazzetto, G. T. Enantioselective Molecular Recognition of Chiral Organic Ammonium Ions and Amino Acids using Cavitand-Salen-Based Receptors. *Eur. J. Org. Chem.* **2011**, *2011*, 5674−5680.
(23) Ravikumar, I.; Ghosh, P. Unusual Recognition of $(N\text{-}Bu_4N)_2SO_4$ by a Cyanuric Acid Based Host via Contact Ion-Pair Interactions. *Chem. Commun.* **2010**, *46*, 6741−6743.
(24) Cametti, M.; Nissinen, M.; Dalla Cort, A.; Mandolini, L.; Rissanen, K. Ion Pair Recognition of Quaternary Ammonium and Iminium Salts by Uranyl-Salophen Compounds in Solution and in the Solid State. *J. Am. Chem. Soc.* **2007**, *129*, 3641−3648.
(25) Molina-Muriel, R.; Aragay, G.; Escudero-Adán, E. C.; Ballester, P. Switching from Negative-Cooperativity to No-Cooperativity in the Binding of Ion-Pair Dimers by a Bis(Calix[4]Pyrrole) Macrocycle. *J. Org. Chem.* **2018**, *83*, 13507−13514.
(26) Gassensmith, J. J.; Arunkumar, E.; Barr, L.; Baumes, J. M.; DiVittorio, K. M.; Johnson, J. R.; Noll, B. C.; Smith, B. D. Self-Assembly of Fluorescent Inclusion Complexes in Competitive Media including the Interior of Living Cells. *J. Am. Chem. Soc.* **2007**, *129*, 15054−15059.
(27) Gassensmith, J. J.; Barr, L.; Baumes, J. M.; Paek, A.; Nguyen, A.; Smith, B. D. Synthesis and Photophysical Investigation of Squaraine Rotaxanes by "Clicked Capping. *Org. Lett.* **2008**, *10*, 3343−3346.
(28) Liu, W.; Oliver, A. G.; Smith, B. D. Macrocyclic Receptor for Precious Gold, Platinum, or Palladium Coordination Complexes. *J. Am. Chem. Soc.* **2018**, *140*, 6810−6813.
(29) Albrecht, M.; Müller, M.; Mergel, O.; Rissanen, K.; Valkonen, A. CH-Directed Anion-Π Interactions in the Crystals of Penta-fluorobenzyl-Substituted Ammonium and Pyridinium Salts. *Chem. - Eur. J.* **2010**, *16*, 5062−5069.
(30) The validity of this binding enhancement effect was supported by an additional titration experiment that added $TBA^+\cdot Cl^-$ to a mixture of **M** and $\mathbf{1}^+\cdot PF_6^-$ and found that $Cl^-$ affinity was increased by a factor of 5 ($K_a$ = 246 $M^{-1}$, Figures S42 and S43).
(31) Jia, C.; Zuo, W.; Yang, D.; Chen, Y.; Cao, L.; Custelcean, R.; Hostaš, J.; Hobza, P.; Glaser, R.; Wang, Y. Y.; et al. Selective Binding of Choline by a Phosphate-Coordination-Based Triple Helicate Featuring an Aromatic Box. *Nat. Commun.* **2017**, *8*, 938.
(32) Hansch, C.; Leo, A.; Taft, R. W. A Survey of Hammett Substituent Constants and Resonance and Field Parameters. *Chem. Rev.* **1991**, *91*, 165−195.
(33) Reinhoudt, D. N.; De Jong, F.; Tomassen, H. P. M. Metal Fluorides as Base for the "Templated" Synthesis of Crown Ethers. *Tetrahedron Lett.* **1979**, *20*, 2067−2070.
(34) Brown, C. L.; Philp, D.; Stoddart, J. F. The Template-Directed Synthesis of a Rigid Tetracationic Cyclophane Receptor. *Synlett* **1991**, *1991*, 462−464.
(35) Marsella, M. J.; Maynard, H. D.; Grubbs, R. H. Template-Directed Ring-Closing Metathesis: Synthesis and Polymerization of Unsaturated Crown Ether Analogs. *Angew. Chem., Int. Ed. Engl.* **1997**, *36*, 1101−1103.
(36) Georgakilas, V.; Gournis, D.; Petridis, D. Organoclay Derivatives in the Synthesis of Macrocycles. *Angew. Chem., Int. Ed.* **2001**, *40*, 4286−4288.
(37) Diederich, F.; Stang, P. J. *Templated Organic Synthesis*; Wiley-VCH: Weinheim, 2000.
(38) Peck, E. M.; Liu, W.; Spence, G. T.; Shaw, S. K.; Davis, A. P.; Destecroix, H.; Smith, B. D. Rapid Macrocycle Threading by a Fluorescent Dye-Polymer Conjugate in Water with Nanomolar Affinity. *J. Am. Chem. Soc.* **2015**, *137*, 8668−8671.
(39) Ashton, P. R.; Philp, D.; Spencer, N.; Stoddart, J. F. A. New Design Strategy for the Self-Assembly of Molecular Shuttles. *J. Chem. Soc., Chem. Commun.* **1992**, 1124−1128.
(40) Ramalingam, V.; Urbach, A. R. Cucurbit[8]Uril Rotaxanes. *Org. Lett.* **2011**, *13*, 4898−4901.
(41) Beer, P. D.; Sambrook, M. R.; Curiel, D. Anion-Templated Assembly of Interpenetrated and Interlocked Structures. *Chem. Commun.* **2006**, 2105−2117.
(42) Since the reaction was performed in a biphasic solvent, the hydrophilic sulfate and ascorbate anions are assumed to remain in the water phase and not affect the binding of **M** with $Q^+\cdot Cl^-$ in chloroform.
(43) Murgu, I.; Baumes, J. M.; Eberhard, J.; Gassensmith, J. J.; Arunkumar, E.; Smith, B. D. Macrocycle Breathing in [2]Rotaxanes with Tetralactam Macrocycles. *J. Org. Chem.* **2011**, *76*, 688−691.


DOI: 10.1021/acs.joc.8b03197
*J. Org. Chem.* 2019, 84, 2808−2816

(44) Gassensmith, J. J.; Matthys, S.; Lee, J. J.; Wojcik, A.; Kamat, P. V.; Smith, B. D. Squaraine Rotaxane as a Reversible Optical Chloride Sensor. *Chem. - Eur. J.* **2010**, *16*, 2916−2921.
(45) Farràs, P.; Escudero-Adán, E. C.; Viñas, C.; Teixidor, F. Controlling the Pirouetting Motion in Rotaxanes by Counterion Exchange. *Inorg. Chem.* **2014**, *53*, 8654−8661.
(46) Fielden, S. D. P.; Leigh, D. A.; McTernan, C. T.; Pérez-Saavedra, B.; Vitorica-Yrezabal, I. J. Spontaneous Assembly of Rotaxanes from a Primary Amine, Crown Ether And Electrophile. *J. Am. Chem. Soc.* **2018**, *140*, 6049−6052.
(47) Thordarson, P. Determining Association Constants from Titration Experiments in Supramolecular Chemistry. *Chem. Soc. Rev.* **2011**, *40*, 1305−1323.
(48) Gassensmith, J. J.; Baumes, J. M.; Eberhard, J.; Smith, B. D. Cycloaddition to an Anthracene-Derived Macrocyclic Receptor with Supramolecular Control of Regioselectivity. *Chem. Commun.* **2009**, 2517−2519.
(49) Stewart, J. J. P. *MOPAC*; Stewart Computational Chemistry: Colorado Springs, CO, 2008.



DOI: 10.1021/acs.joc.8b03197
*J. Org. Chem.* 2019, 84, 2808−2816